



DIGITAL ACCESS TO SCHOLARSHIP AT HARVARD

Coupling of Silicon-Vacancy Centers to a Single Crystal Diamond Cavity

The Harvard community has made this article openly available.
[Please share](#) how this access benefits you. Your story matters.

Citation	Lee, Jonathan C., Igor Aharonovich, Andrew P. Magyar, Fabian Rol, and Evelyn L. Hu. 2012. Coupling of silicon-vacancy centers to a single crystal diamond cavity. <i>Optics Express</i> 20(8): 8891.
Published Version	doi:10.1364/OE.20.008891
Accessed	February 19, 2015 1:12:11 PM EST
Citable Link	http://nrs.harvard.edu/urn-3:HUL.InstRepos:11006841
Terms of Use	This article was downloaded from Harvard University's DASH repository, and is made available under the terms and conditions applicable to Open Access Policy Articles, as set forth at http://nrs.harvard.edu/urn-3:HUL.InstRepos:dash.current.terms-of-use#OAP

(Article begins on next page)

Coupling of silicon-vacancy centers to a single crystal diamond cavity

Jonathan C. Lee,* Igor Aharonovich, Andrew P. Magyar, Fabian Rol,
and Evelyn L. Hu

*School of Engineering and Applied Sciences, Harvard University, Cambridge, Massachusetts,
02138, USA.*

*jclee@seas.harvard.edu

Abstract: Optical coupling of an ensemble of silicon-vacancy (SiV) centers to single-crystal diamond microdisk cavities is demonstrated. The cavities are fabricated from a single-crystal diamond membrane generated by ion implantation and electrochemical liftoff followed by homo-epitaxial overgrowth. Whispering gallery modes spectrally overlap with the zero-phonon line (ZPL) of the SiV centers and exhibit quality factors ~ 2200 . Lifetime reduction from 1.8 ns to 1.48 ns is observed from SiV centers in the cavity compared to those in the membrane outside the cavity. These results are pivotal in developing diamond integrated photonics networks.

© 2012 Optical Society of America

OCIS codes: (140.4780) Optical resonators;(140.3945) Microcavities; (160.2220) Defect-center materials.

References and links

1. C. Kurtsiefer, S. Mayer, P. Zarda, and H. Weinfurter, "Stable Solid-State source of single photons," *Phys. Rev. Lett.* **85**, 290–293 (2000).
2. P. Neumann, J. Beck, M. Steiner, F. Rempp, H. Fedder, P. R. Hemmer, J. Wrachtrup, and F. Jelezko, "Single-Shot readout of a single nuclear spin," *Science* **329**, 542–544 (2010).
3. B. B. Buckley, G. D. Fuchs, L. C. Bassett, and D. D. Awschalom, "Spin-Light coherence for Single-Spin measurement and control in diamond," *Science* **330**, 1212–1215 (2010).
4. E. Togan, Y. Chu, A. S. Trifonov, L. Jiang, J. Maze, L. Childress, M. V. G. Dutt, A. S. Sorensen, P. R. Hemmer, A. S. Zibrov, and M. D. Lukin, "Quantum entanglement between an optical photon and a solid-state spin qubit," *Nature* **466**, 730–734 (2010).
5. E. Neu, D. Steinmetz, J. Riedrich-Möller, S. Gsell, M. Fischer, M. Schreck, and C. Becher, "Single photon emission from silicon-vacancy colour centres in chemical vapour deposition nano-diamonds on iridium," *New J. Phys.* **13**, 025012 (2011).
6. I. Aharonovich, S. Castelletto, B. Johnson, J. McCallum, D. Simpson, A. Greentree, and S. Prawer, "Chromium single-photon emitters in diamond fabricated by ion implantation," *Phys. Rev. B* **81**, 121201 (2010).
7. J. R. Rabeau, Y. L. Chin, S. Prawer, F. Jelezko, T. Gaebel, and J. Wrachtrup, "Fabrication of single nickel-nitrogen defects in diamond by chemical vapor deposition," *Appl. Phys. Lett.* **86**, 131926 (2005).
8. N. Gisin, G. Ribordy, W. Tittel, and H. Zbinden, "Quantum cryptography," *Rev. Mod. Phys.* **74**, 145–195 (2002).
9. J. P. Goss, R. Jones, S. J. Breuer, P. R. Briddon, and S. Öberg, "The Twelve-Line 1.682 eV luminescence center in diamond and the Vacancy-Silicon complex," *Phys. Rev. Lett.* **77**, 3041–3044 (1996).
10. I. Aharonovich, A. D. Greentree, and S. Prawer, "Diamond photonics," *Nat. Photon.* **5**, 397–405 (2011).
11. C. Santori, P. E. Barclay, K. C. Fu, R. G. Beausoleil, S. Spillane, and M. Fisch, "Nanophotonics for quantum optics using nitrogen-vacancy centers in diamond," *Nanotechnology* **21**, 274008 (2010).
12. A. Faraon, P. E. Barclay, C. Santori, K. C. Fu, and R. G. Beausoleil, "Resonant enhancement of the zero-phonon emission from a colour centre in a diamond cavity," *Nat. Photon.* **5**, 301–305 (2011).
13. P. Barclay, K. Fu, C. Santori, A. Faraon, and R. Beausoleil, "Hybrid nanocavity resonant enhancement of color center emission in diamond," *Phys. Rev. X* **1**, 011007 (2011).
14. T. M. Babinec, H. J. M., M. Khan, Y. Zhang, J. R. Maze, P. R. Hemmer, and M. Loncar, "A diamond nanowire single-photon source," *Nat. Nano.* **5**, 195–199 (2010).

15. J. Wolters, A. W. Schell, G. Kewes, N. Nüsse, M. Schoengen, H. Döscher, T. Hannappel, B. Löchel, M. Barth, and O. Benson, "Enhancement of the zero phonon line emission from a single nitrogen vacancy center in a nanodiamond via coupling to a photonic crystal cavity," *Appl. Phys. Lett.* **97**, 141108 (2010).
16. D. Englund, B. Shields, K. Rivoire, F. Hatami, J. Vučković, H. Park, and M. D. Lukin, "Deterministic coupling of a single nitrogen vacancy center to a photonic crystal cavity," *Nano Lett.* **10**, 3922–3926 (2010).
17. T. van der Sar, J. Hagemeyer, W. Pfaff, E. C. Heeres, S. M. Thon, H. Kim, P. M. Petroff, T. H. Oosterkamp, D. Bouwmeester, and R. Hanson, "Deterministic nanoassembly of a coupled quantum emitter-photonic crystal cavity system," *Appl. Phys. Lett.* **98**, 193103 (2011).
18. B. A. Fairchild, P. Olivero, S. Rubanov, A. D. Greentree, F. Waldermann, R. A. Taylor, I. Walmsley, J. M. Smith, S. Huntington, B. C. Gibson, D. N. Jamieson, and S. Praver, "Fabrication of ultrathin Single-Crystal diamond membranes," *Adv. Mater.* **20**, 4793–4798 (2008).
19. I. Bayn, B. Meyler, J. Salzman, and R. Kalish, "Triangular nanobeam photonic cavities in single-crystal diamond," *New J. Phys.* **13**, 025018 (2011).
20. C. F. Wang, R. Hanson, D. D. Awschalom, E. L. Hu, T. Feygelson, J. Yang, and J. E. Butler, "Fabrication and characterization of two-dimensional photonic crystal microcavities in nanocrystalline diamond," *Appl. Phys. Lett.* **91**, 201112 (2007).
21. C. P. Michael, K. Srinivasan, T. J. Johnson, O. Painter, K. H. Lee, K. Hennessy, H. Kim, and E. Hu, "Wavelength- and material-dependent absorption in GaAs and AlGaAs microcavities," *Appl. Phys. Lett.* **90**, 051108 (2007).
22. A. P. Magyar, J. C. Lee, A. M. Limarga, I. Aharonovich, F. Rol, D. R. Clarke, M. Huang, and E. L. Hu, "Fabrication of thin, luminescent, single-crystal diamond membranes," *Appl. Phys. Lett.* **99**, 081913 (2011).
23. I. Aharonovich, J. C. Lee, A. P. Magyar, B. B. Buckley, C. G. Yale, D. D. Awschalom, and E. L. Hu, "Homoepitaxial growth of single crystal diamond membranes for quantum information processing," *Adv. Mater.* **24**, OP54–OP59 (2012).
24. C. Lee, E. Gu, M. Dawson, I. Friel, and G. Scarsbrook, "Etching and micro-optics fabrication in diamond using chlorine-based inductively-coupled plasma," *Diamond Relat. Mater.* **17**, 1292–1296 (2008).
25. H. Sternschulte, K. Thonke, R. Sauer, P. C. Münzinger, and P. Michler, "1.681-eV luminescence center in chemical-vapor-deposited homoepitaxial diamond films," *Phys. Rev. B* **50**, 14554–14560 (1994).
26. C. D. Clark, H. Kanda, I. Kiflawi, and G. Sittas, "Silicon defects in diamond," *Phys. Rev. B* **51**, 16681–16688 (1995).
27. A. V. Turukhin, C. Liu, A. A. Gorokhovskiy, R. R. Alfano, and W. Phillips, "Picosecond photoluminescence decay of si-doped chemical-vapor-deposited diamond films," *Phys. Rev. B* **54**, 16448–16451 (1996).
28. A. C. Tamboli, M. C. Schmidt, A. Hirai, S. P. DenBaars, and E. L. Hu, "Observation of whispering gallery modes in nonpolar m-plane GaN microdisks," *Appl. Phys. Lett.* **94**, 251116 (2009).
29. J. Riedrich-Möller, L. Kipfstuhl, C. Hepp, E. Neu, C. Pauly, F. Mücklich, A. Baur, M. Wandt, S. Wolff, M. Fischer, S. Gsell, M. Schreck, and C. Becher, "One- and two-dimensional photonic crystal microcavities in single crystal diamond," *Nat. Nano.* **7**, 69–74 (2011).

Color centers in diamond have emerged as leading candidates for solid state quantum information processing (QIP) due to their unique physical properties such as single photon emission at room temperature [1–4]. Intense research efforts on individual color centers in diamond over the past decade have yielded significant insights into the photo-physics of defects in diamond. In particular, there is a growing interest in utilizing color centers that exhibit a narrow luminescence band, short excited state lifetime, and single photon emission at room temperature [5–7]. Such defects are extremely attractive photon sources for quantum key distribution or optical quantum computation [8]. One example of such a defect is the SiV center, consisting of a single silicon atom in the split vacancy configuration with a ZPL transition at 738 nm [9] as shown in Fig. 1(a) and Fig. 1(b).

Significant emphasis has been devoted to the coupling of emitters to optical cavities to facilitate the control of emission properties while guiding light into a photonic network [10–17]. However, a major challenge to achieving diamond-based quantum photonics is the difficulty in processing single-crystal diamond for the fabrication of optical cavities coupled to its color centers. Indeed, fabricating such cavities from bulk single crystal diamond by ion implantation degrades the optical properties of the embedded color centers impeding their use for photonic platforms [18, 19]. Furthermore, earlier work has shown that using nanocrystalline diamond to form optical cavities places limits on the quality factors of those cavities [20]. Even for epitaxial material systems where very high quality factors ($> 10^5$) have been demonstrated, subtle vari-

ations in materials quality and absorption are found to still limit the Q obtainable [21]. Thus, it is critical to form high quality optical cavities from single crystal diamond, but this in turn poses additional challenges.

This work addresses some of those challenges through the formation of high quality, optically thin, single crystal diamond films incorporating SiV centers formed by epitaxial overgrowth on a single crystal membrane. Microdisk cavities were subsequently fabricated from the material, demonstrating quality factors in the range of 2000-3000. Cavity-mediated reduction of the fluorescence lifetime of the SiV centers was also measured.

The starting material was a type II-a CVD diamond sample with nitrogen concentration less than 1 ppm, obtained from Element-Six. Diamond membranes, 1.7 μm thick, were generated using ion implantation followed by thermal annealing and an electrochemical etch process [22]. The membranes were cleaned using a mixed (1:1:1 sulfuric:perchloric:nitric acid) boiling acid bath, and then transferred onto a 2 μm thick silicon dioxide layer on top of silicon, which provides optical isolation and allows independent optical characterization of the diamond membranes. Photoluminescence (PL) from the diamond membranes showed no optical signatures of the SiV centers. A short epitaxial over-growth (~ 200 nm) was employed using a microwave plasma chemical vapor deposition (MPCVD) reactor to introduce the SiV centers [23]; the surface roughness is 3 nm after the regrowth. The overgrown material is grown epitaxially, and forms a complete single crystal. Neither polycrystalline material nor grain boundaries have been observed in our membranes by inspecting it with a scanning electron microscope (SEM). The composite structure was flipped so that the original template is the top surface. The structure was thinned using argon-chlorine-based inductively coupled plasma reactive ion etching (ICP RIE) to first smooth the surface [24], followed by an oxygen-based ICP RIE to thin the structure to ~ 500 nm thick. Thus, the resulting structure is a composite diamond membrane composed of 300 nm of the original membrane template and 200 nm of the overgrown material. The schematic of the fabrication process is depicted in Fig. 1(c).

A reduced Raman linewidth was measured from the overgrown layer (full width half maximum (FWHM): ~ 3 cm^{-1}) compared to the original diamond template (FWHM: ~ 9 cm^{-1}) indicating the better material quality of the overgrown layer. Figure 2(a) shows the room temperature PL spectra of the diamond membrane before thinning (blue curve) and after the removal of ~ 1.4 μm (green curve) and ~ 1.6 μm (red curve) of the original diamond template. Broadband luminescence obscured the luminescence of SiV centers before the membrane is thinned (Fig. 2(a) blue curve). The broadband luminescence is further reduced through the removal of the original diamond template (Fig. 2(a) green and red curves). A pronounced ZPL at 738 nm attributed to the SiV is clearly seen after most of the original template was etched away. The FWHM of the ZPL was measured to be ~ 6 nm at room temperature. At low temperature (18 K) the FWHM was reduced to ~ 3 nm (Fig. 2(b), however, the fine structure of the defect (Fig. 1(b)) was not resolved [25, 26] due to a high concentration of the emitters and their inhomogeneous broadening due to the strain fields.

Microdisk cavities were made from the 500 nm thick diamond membrane after epitaxial overgrowth and ICP-RIE thinning. An 80 nm thick silicon dioxide hard mask was deposited using plasma-enhanced chemical vapor deposition (PECVD). The 2.5 μm diameter microdisks were patterned using a 100 KeV electron beam lithography system (Elionix) with poly (methyl methacrylate) (PMMA) as the resist. The patterns were then transferred by a fluorine based ICP-RIE step to etch into the silicon dioxide hard mask, followed by a oxygen based ICP-RIE step to transfer the pattern to the diamond membrane. Figure 2(c) shows a SEM image of the diamond microdisk cavity with a diameter of 2.5 μm and a thickness of 500 nm. Finite difference time domain (FDTD) simulation of the field intensity (H_z) profile of a zeroth order whispering gallery mode (WGM) in the radial direction with transverse electric (TE) polarization is shown

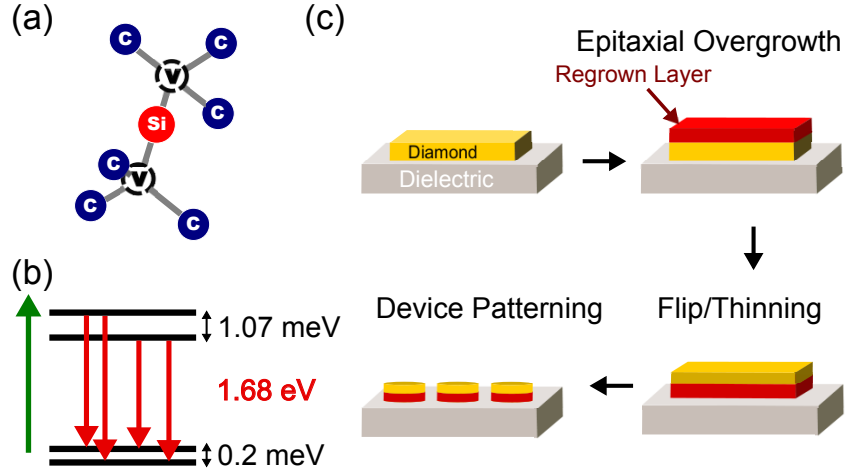


Fig. 1. (a) Schematic of the SiV defect structure in diamond. The red atom represents the silicon, the empty circle represents the surrounding vacancies and the blue atoms are the carbon atoms. (b) The energy level diagram of SiV centers with doublets in both the ground states and excited states. The emitter can be excited by a 532 nm excitation and the emission is centered near the ZPL at 738 nm. (c) Fabrication process of the cavity. A $\sim 1.7 \mu\text{m}$ thick diamond membrane is placed on a silicon-dioxide substrate followed by epitaxial overgrowth of a thin diamond film. The film is flipped and thinned using reactive ion etching and the microdisk cavities are patterned using e-beam lithography with silicon-dioxide as a hard mask.

in Fig. 2(d). The modal volume of the mode is $\sim 0.273 \mu\text{m}^3$ ($9.6 (\lambda/n)^3$). The WGMs radiate preferentially in the x-y plane. Figure 2(e) shows the room temperature micro-PL measurements recorded from the $2.5 \mu\text{m}$ diameter disk. The PL measurements were performed with a confocal microscope (LabRAM ARAMIS, Horiba Jobin-Yvon) with 532 nm laser excitation. The excitation and signal collection went through the same objective with NA = 0.9 and magnification $100\times$ which results in spatial resolution $\sim 1 \mu\text{m}$. By comparing the free spectral range of the WGMs to the FDTD simulations (Lumerical Solutions, Inc), the polarization and the order (both radial and azimuthal direction) of the WGMs are identified. Quality factors, Q, of these modes were determined to be ~ 2200 by calculating $\frac{\lambda_{cav}}{\Delta\lambda_{cav}}$, where λ_{cav} is the cavity mode wavelength and $\Delta\lambda_{cav}$ is the FWHM of the mode.

A high resolution spectrum of the TE mode centered at 736.5 nm is shown in Fig 3(a). The mode is found to be zeroth order in the radial direction ($\text{TE}_0^{m=20}$) with $Q \sim 2200$ and overlaps spectrally with the SiV ZPL emission. To investigate the emitter-cavity system further, lifetime measurements were performed. A frequency-doubled pulsed Ti:Sapphire laser at 460 nm with a 76 MHz repetition rate and pulse width less than 70 femtoseconds was used to excite the SiV emitters. The 18K measurement was made with the sample in a cryostat (Janis) with excitation and signal collection passing through the same NA = 0.5 objective, with $100\times$ magnification and 1 mW laser excitation power. The laser light was reflected by a dichroic mirror and the collected PL signal was filtered by a band pass filter ($747 \text{ nm} \pm 17 \text{ nm}$) and directed onto an avalanche photo-diode (Micro Photonic Devices, jitter time $\sim 50 \text{ ps}$). The spectral window includes both the enhanced part and non-enhanced luminescence from the SiV centers. The cavity mode linewidth is $\sim 0.336 \text{ nm}$ and the linewidth of the SiV ZPL is $\sim 3 \text{ nm}$. Therefore, we approximated $\sim 10\%$ of the SiV centers are coupled to the cavity modes, taking into account that the Debye-Waller factor is $\sim 80\%$ as reported in the literature [5]. The results of the lifetime

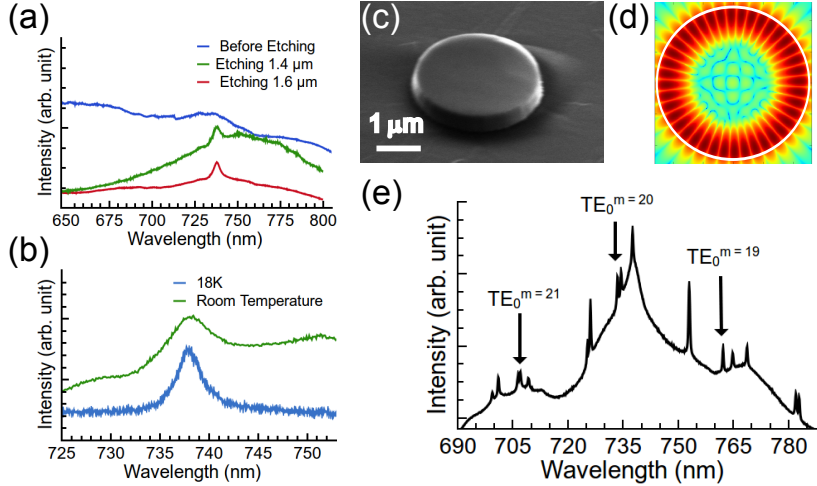


Fig. 2. (a) Room temperature PL curves recorded from the membrane immediately after regrowth (blue curve), after a subsequent removal of $\sim 1.4 \mu\text{m}$ of the original template (green curve) and a final thinning to 300 nm thick membrane (100nm:200nm original template:overgrown layer). A pronounced ZPL from the SiV centers was observed as the original template is removed. The FWHM of the ZPL is $\sim 6 \text{ nm}$. (b) Low temperature PL measurement recorded from the membrane after removal of $\sim 1.4 \mu\text{m}$ of the original membrane. The FWHM of the ZPL of SiV centers at 9 K is $\sim 3 \text{ nm}$. (c) SEM image of a $2.5 \mu\text{m}$ diameter micro-disk cavity fabricated from single-crystal diamond. (d). FDTD simulation of the field intensity (H_z) profile in log scale for the TE mode with zeroth order in radial direction ($\text{TE}_0^{m=20}$). The red color indicates higher field intensity, and the white circle indicates the periphery of the micro-disk. (e) Room temperature PL spectrum recorded from the microdisk cavity with $20 \mu\text{W}$ laser excitation. The WGMs are observed. The zeroth order radial TE mode has a Q of ~ 2000 .

measurements are shown in Fig. 3(b) and are best fit with a bi-exponential decay. The lifetime of the SiV centers coupled to the microdisk is measured to be $\sim 1.48 \pm 0.04 \text{ ns}$ while the lifetime measured from the membrane outside of the disk is $\sim 1.83 \pm 0.09 \text{ ns}$. The second part of the bi-exponential fit accounts for the fast decays which is measured $0.66 \pm 0.02 \text{ ns}$ from the membrane, and $0.43 \pm 0.01 \text{ ns}$ from the cavity due to other defects in the membranes. The lifetime reduction is in reference to a diamond membrane having the same thickness and having undergone exactly the same fabrication process as the microdisk cavities. Hence, other reasons for lifetime reduction, e.g. non radiative channels or surface defects, if present, would be the same in both the membrane and the microdisk. Therefore, we believe that the only reason for the observed lifetime reduction is the modification of the density of states of the emitters due to coupling to the cavity modes. The Purcell enhancement based on lifetime modification is estimated to be ~ 1.3 . The reduced lifetime value can be regarded as an averaged lifetime of multiple different exponential decay curves, which represent different SiV centers in the disk coupled to the cavity mode. Additionally, an enhanced photon count rate from the avalanche photo diode (APD) was observed from the microdisk ($\sim 40,000 \text{ counts/s}$) compared to the diamond membrane ($\sim 3000 \text{ counts/s}$) under identical excitation conditions. The microdisk cavity can increase the far-field collection through geometrical effects that enhance photon extraction and scattering from the disk. Thus the lifetime provides a more accurate picture of the cavity enhancement of the emitters while the enhanced collection rate results from a combination of increased collection efficiency and enhanced spontaneous emission from SiV

centers.

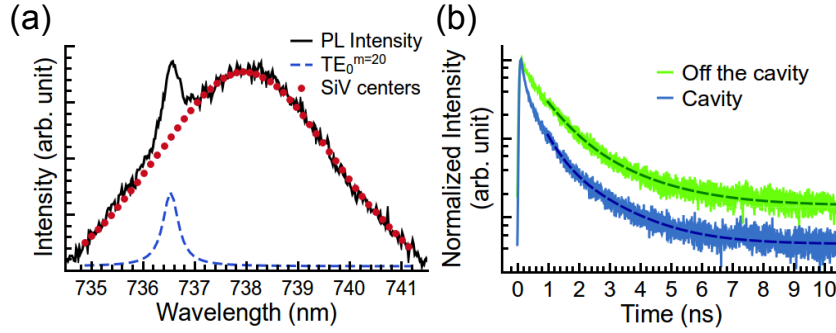


Fig. 3. (a) Room temperature PL spectrum of the 1st order radial TE mode ($TE_0^{m=20}$). The spectrum is background corrected. The Q factor is ~ 2200 and spectral overlap with the ZPL of SiV centers was observed. The solid curve is the spectrum measured, the dashed curve is a Lorentzian fit of the cavity mode, and the dotted curve is a Lorentzian fit of the ZPL of SiV center. (b) Fluorescence lifetime measurement of SiV centers within microdisk resonators shows lifetime reduction from 1.83 ns to 1.48 ns, compared to the SiV centers in the diamond membrane, recorded at 18 K. The lifetime was fit to a bi-exponential decay (dashed lines) where reduction for both the fast and slow decay channel were observed.

The quality factors of ~ 2200 measured from the microdisks are comparable with values recently reported for a single crystal diamond micro-ring resonator [12] and a significantly higher value than devices made of nanocrystalline diamond [20] or milled by using a focused ion beam [19]. Examination of the PL data of Fig. 2(a) shows the SiV peak sitting atop a broad band of luminescence, which is successively diminished as the composite diamond membrane is thinned. The broad band luminescence is likely due to other impurities within the membrane and could lead to material reabsorption and hence limit the Q of the cavity. Removal of that central region may also provide an increase in the observed Q as has been seen in other material systems [28].

Coupling of SiV defects to an optical cavity marks pivotal progress towards the realization of scalable diamond-based quantum photonics networks. Although demonstrated with an ensemble in this work, coupling of single emitters should also be possible using the techniques described here. Our approach enables the formation of optically thin single crystal membranes with good optical and structural properties. Such membranes can serve as the basis for microdisks and photonic crystal cavities as well as enable the construction of an integrated photonic network of coupled diamond cavities and waveguides. The approach provides flexibility in both the formation of color centers, as well as flexibility in the geometry of optical cavities formed around those centers. We believe that further optimization of the fabrication steps, such as the use of high temperature annealing or further reduction of impurity absorption will produce high Qs and stronger emitter-cavity coupling. These initial results represent an important milestone in the achievement of diamond-based cavity quantum electrodynamics.

Acknowledgments

The authors acknowledge the help of D.R. Clarke for access to the PL and Raman facilities, and M. Huang for assistance with ion implantation. The authors also thank K.J. Russell, T.L. Liu, T.M. Babinec, A.L. Falk, H.J. Heremans, B.B. Buckley, C.G. Yale and D.D. Awschalom for useful discussions. This work was carried out with the financial support of DARPA under the Quantum Entanglement Science and Technology (QuEST) Program. This work was enabled

by facilities available at the Center for Nanoscale Systems (CNS), a member of the National Nanotechnology Infrastructure Network (NNIN), which is supported by the National Science Foundation under NSF award no. ECS-0335765. CNS is part of the Faculty of Arts and Sciences at Harvard University. At the time of manuscript preparation a related preprint appeared, which describes coupling of SiV to photonic crystal cavities [29].